NANO LETTERS

2004
Vol. 4, No. 1
137−142

Ion Transport in Nanofluidic Channels

Hirofumi Daiguji,*,† Peidong Yang,‡,§ and Arun Majumdar§,||

Institute of Environmental Studies, Graduate School of Frontier Sciences, The University of Tokyo, Tokyo 113-0033, Japan, Department of Chemistry, University of California, Berkeley, California, Materials Science Division, Lawrence Berkeley National Laboratory, Berkeley, California, and Department of Mechanical Engineering, University of California, Berkeley, California

Received September 24, 2003; Revised Manuscript Received November 3, 2003

ABSTRACT

Theoretical modeling of ionic distribution and transport in silica nanotubes, 30 nm in diameter and 5 μm long, suggest that when the diameter is smaller than the Debye length, a unipolar solution of counterions is created within the nanotube and the coions are electrostatically repelled. By locally modifying the surface charge density through a gate electrode, the ion concentration can be depleted under the gate and the ionic current can be significantly suppressed. It is proposed that this could form the basis of a unipolar ionic field-effect transistor.

Introduction. Ion transport in nanoscale channels has recently received increasing attention. Much of that has resulted from experiments that report modulation of ion transport through the protein ion channel, α-hemolysin, due to passage of single biomolecules of DNA or proteins.[1−3] This has prompted research toward fabricating synthetic nanopores out of inorganic materials and studying biomolecular transport through them.[4] Recently, Fan et al.[5] reported the synthesis of arrays of silica nanotubes with internal diameters in the range of 5−100 nm and with lengths 1−20 μm (see Figure 1). While it is difficult to control the internal structure and chemistry of synthetic nanotubes as precisely as that of α-hemolysin and other biological ion channels, nanotubes do offer an aspect ratio that is much higher than that of protein ion channels. The fact that the nanotube lengths fall within the resolution of optical microscopy and optical lithography opens the possibility of imaging transport of single biomolecules through the nanotube while controlling the charge distribution on the nanotube surface by external microfabricated electrodes. This would allow new ways of detecting and manipulating single biomolecules. To achieve this, however, it is critical to understand the ionic conditions and ion transport inside the nanotube. In view of this, the purpose of the present study is to study the nature of ion transport through a silica nanotube under an external bias and investigate the effects of the surface charge density.

It must be noted that in most of the cases considered here, the internal diameter of the nanotubes is in the range of or smaller than the Debye length for the ions ($l_D \approx 1-100$ nm). Therefore, the phenomena studied here are significantly different from that in microfluidic devices, which are invariably larger than the Debye length.[6−8] In microfluidic devices, electroosmotic flow is studied as a means to generate fluid flow for pumping and biomolecular separation, but not generally to control ionic current. If, however, the surface of a channel is charged and the height of a channel is less than the Debye length, ionic current can be controlled as well. The purpose of the present study is develop a model to design inorganic nanopores and nanotubes in order to have controlled ion transport, and then study the effects of biomolecules on ion current, similar to that occurring in protein nanopores such as α-hemolysin.

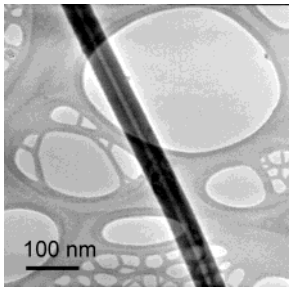

Figure 1. TEM of silica nanotube with internal diameter of about 10 nm.[5]

Governing Equations. The first simplification in the calculation of ionic current is in the modeling of the "Stern layer", the compact electric double layer adjacent to a charged surface. For low surface charge density, the layer of counterions extends well beyond the surface (diffuse layer). However, for high surface charge density, regardless of the concentration distribution away from a surface, most

* Corresponding author. E-mail: daiguji@k.u-tokyo.ac.jp; Tel: +81-3-5841-8587; Fax: +81-3-3818-0835
† The University of Tokyo.
‡ Department of Chemistry, University of California.
§ Lawrence Berkeley National Laboratory.
|| Department of Mechanical Engineering, University of California.

10.1021/nl0348185 CCC: $27.50
Published on Web 11/22/2003

of the counterions that effectively balance the surface charge are located in the first few angstroms from the surface.[9,10] For the structural and dynamical properties of the ions within the Stern layer, there are a number of theoretical studies,[11,12] but there are still open questions. Here we assume that inside the Stern layer the ions are rigidly held and they do not contribute to the ionic current. If so, we do not need to calculate the contribution from the Stern layer. The wall can be regarded as the interface between the Stern layer and the diffuse layer, and the surface charge density here is that of the wall plus that of ions within the Stern layer.

The second simplification is that only the current due to the electrophoresis is considered. In general, the ionic current is generated by electrophoresis and electroosmosis. When the height of a channel is smaller than the Debye length, the ionic current due to electrophoresis is dominant. But as the surface charge density increases, the ionic current due to electroosmosis increases and it cannot be neglected. We address this issue in the Appendix and show when electroosmosis can be neglected.

In the present study, the Poisson−Nernst−Planck (PNP) equations are used to calculate ionic current across a channel. The PNP theory of electrodiffusion has been applied to liquid junctions and membrane electrochemistry.[13−15] The PNP equations consist of the Poisson equation (eq 1) and the Nernst−Planck equations (eq 2) for all ionic species moving through the channel. The electrostatic potential ϕ is calculated with the Poisson equation

$$\nabla^2\phi = -\frac{1}{\epsilon_0\epsilon}\sum_a z_a e n_a \tag{1}$$

where ϵ_0 is the permittivity of vacuum, ϵ is the dielectric constant of solution, n_a is the number density of ions of species a, and $z_a e$ is their charge. The flux $\boldsymbol{J}_a$ due to an ion species a is provided by Nernst−Planck equation, which combines the diffusion due to a concentration gradient with that from a potential gradient

$$\boldsymbol{J}_a = -D_a\left(\nabla n_a + \frac{z_a e n_a}{kT}\nabla\phi\right) \tag{2}$$

where D_a is the diffusivity of ion species a. We are interested in steady-state solution, which satisfies the continuity equation $\nabla\cdot\boldsymbol{J}_a = 0$, or equivalently:

$$\nabla\cdot\left(\nabla n_a + \frac{z_a e n_a}{kT}\nabla\phi\right) = 0 \tag{3}$$

The boundary conditions for the Poisson equation are given by

$$\nabla\phi = -\frac{\sigma}{\epsilon_0\epsilon} \tag{4}$$

where σ is the surface charge density. The boundary condition for the flux equation is zero current through the wall, i.e., $\boldsymbol{J}_a = 0$. The PNP equations (1) and (3) are solved simultaneously using a finite difference algorithm, yielding the electric potential and ionic density profiles in the system.[16,17] If the electric potential and ionic density profiles are known, the flux $\boldsymbol{J}_a$ due to an ion species a is calculated with eq 2 and the ionic current is obtained by the following equation:

$$\boldsymbol{I}_a = z_a e \int \boldsymbol{J}_a \, \mathrm{d}S \tag{5}$$

where S is a cross-sectional area of the channel. In this study, KCl aqueous solutions were used. The dielectric constant of KCl aqueous solution, ϵ, is 80, the diffusivities of of K^+ and Cl^-, D_{K^+} and D_{Cl-}, are 1.96×10^{-9} and 2.03×10^{-9} m^2/s, respectively.[18]

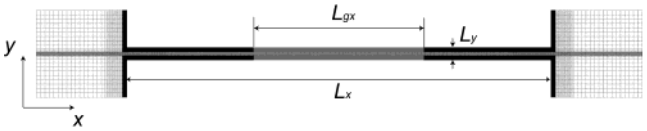

Figure 2. Computational grid (316 × 45) inside a silica nanotube with height of 30 nm, length of 5 μm with 1 μm × 1 μm reservoirs on either side. The gate is centered along the length of the nanotube with a length, $L_{gx} = 2$ μm.

Calculation System. Figure 2 shows the 2D domain for the calculation, where the total length of the channel L_x is 5 μm and the height, L_y, is 30 nm. Reservoirs 1 μm × 1 μm, 2 μm × 2 μm, and 3 μm × 3 μm in size are considered on either side of the channel. We found that the predictions of ion transport depend marginally on the reservoir size, although the basic trends and conclusions in this paper do not change with reservoir size. Hence, predictions for reservoir size 1 μm × 1 μm are presented in this paper. A gate electrode is located at the center of the channel and the length L_{gx} is 2 μm. The surface charge density inside the channel ranged from 0 to -2×10^{-3} C/m^2, whereas the surface charge density at the gate is different from that of other parts due to the presence of the gate electrode. The electric potentials and ionic densities at the boundaries are given by constant values, except for the walls of the channel. The boundary conditions at the walls are given by eq 4 and $\boldsymbol{J}_a = 0$. The surface charge densities at the walls that face the reservoirs are zero. The grid spacing (see Figure 2) outside the channel is 50 nm, whereas the minimum grid spacing of 10 nm is assumed in the x direction near the inlets and outlets of the channel, as well as the gate. The minimum grid spacing in the y direction is inside the channel and the value is 2 nm. The bulk concentration of KCl aqueous solution varies from 10^{-4} to 10^{-2}M.

Calculation Results. *Calibration of 2D PNP Code.* To calibrate the accuracy of the 2D PNP code, the potential and ionic density profiles in the x and y directions were verified separately. These profiles in the y direction were checked using the 1D system of which two negatively charged surfaces of surface charge density $\sigma = -10^{-3}$ C/m^2 are separated by a distance $L_y = 0.5$ μm in a KCl aqueous solution.

When two surfaces are far apart, each surface can be regarded as an isolated surface and the surface potential ϕ_i at an isolated surface of charge density σ is given by the Grahame equation:[19]

$$\phi_i = \frac{2kT}{e}\sinh^{-1}\left[\frac{\sigma}{(8\epsilon\epsilon_0 kTn_{\mathrm{KCl0}})^{1/2}}\right] \tag{6}$$

where n_{KCl0} is the number density of KCl in the bulk solution. The PNP equations were solved numerically using a grid spacing of 2 nm for three different concentrated solutions, 10^{-4}, 10^{-3}, and 10^{-2} M. The surface potentials calculated with the PNP equations are -39.5, -13.7, and -4.56 mV, respectively. In comparison, those calculated with the Grahame equation are -39.5, -13.5, and -4.34 mV, respectively, which indicate excellent agreement.

For a channel without surface charge, the distributions of the electric potential and ionic density in the *y* direction are negligible and the system can be approximated as a 1D system in the *x* direction. In eq 2, the gradient of ionic density in the *x* direction can be assumed to be zero, whereas that for the electric potential can be assumed to be the constant value of $\Delta\phi/L_x$. Hence, the flux can be calculated as

$$\boldsymbol{J}_a = -D_a\left(\frac{z_a e n_{a0}\Delta\phi}{kT \quad L_x}\right) \tag{7}$$

where n_{a0} is the number density of *a* species in the bulk solution and $\Delta\phi$ is the potential bias. When the bulk concentration of KCl aqueous solution is 10^{-4} M and the potential bias is 5 V, the ionic currents of K^+ and Cl^- calculated with eqs 5 and 7 are 21.9 and 22.7 μA/m, respectively. The corresponding calculation results with the PNP equations are 20.9 and 21.7 μA/m, respectively, again indicating agreement within 5%.

Absence of Gate Effect. Before considering the gate effect, to clarify the nature of ion transport in nanofluidic channels, the following three effects were studied: (a) applied bias; (b) surface charge density; (c) bulk ion concentration.

(a) Effect of Applied Bias. Consider the concentration of KCl aqueous solution to be 10^{-4} M and the surface charge density is -10^{-3} C/m^2. The potential at left reservoir is 0 V and the potential at right reservoir varied from 0 to 5 V at an interval of 1 V. Figure 3a shows the electric potential and ionic density profiles in the *x* direction along the axis of symmetry. Inside the channel the difference in ionic density between K^+ and Cl^- is determined by the surface charge density. From the requirement of overall electroneutrality, the difference in ionic density, Δn, is given by

$$\Delta n = -\frac{2\sigma}{eL_y} \tag{8}$$

When the surface charge density is -10^{-3} C/m^2 and the height of the channel is 30 nm, the difference $\Delta n = 4.17 \times 10^{23}$ m^{-3} and the equivalent concentration is 0.69 mM. In Figure 3a, the concentration difference between K^+ and Cl^-

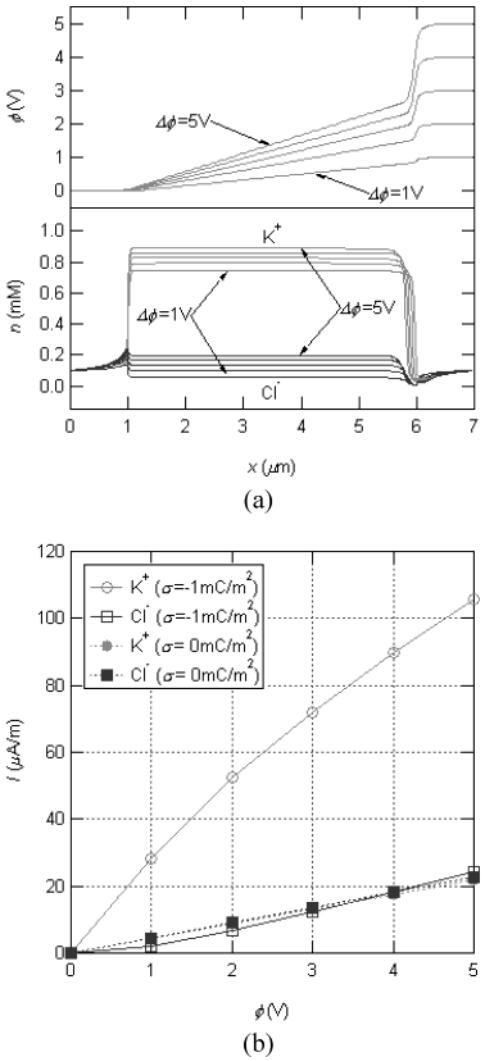

Figure 3. For surface charge density, $\sigma = -10^{-3}$ C/m^2 on the tube surface the effect of potential bias on (a) electric potential profiles along the axis of the channel (top) and ionic density profiles (bottom) in the *x* direction for five different potential biases; (b) current−potential ($I-\phi$) characteristics of the charged channel of (solid lines) and the no charged channel (dashed lines). The bulk concentration of KCl aqueous solution is assumed to be 10^{-4} M.

inside the channel is about 0.69 mM in all cases independent of the potential bias. If the bulk concentration is less than Δn, there exists a large potential barrier for the Cl^- ions to enter the channel, and the channel becomes essentially a "unipolar" solution of K^+ ions that neutralize the negative surface charge. As the potential bias increases, more ions are accumulated inside the channel, although the potential jump at $x = 6$ μm increases and the electric field strength inside the channel does not increase proportionally. Based on the gradients of electric potential and ion concentration, one can use eq 2 to calculate the ionic current. The current−potential ($I - \phi$) characteristics of the channel with and without surface charge are shown in Figure 3b. The $I - \phi$ characteristics for $\sigma = 0$ are almost linear and almost equal for K^+ and Cl^-. For charged channels the $I - \phi$ characteristics are nonlinear because of the fact that the potential gradient inside the channel does not increase proportionally to increasing applied potential difference.

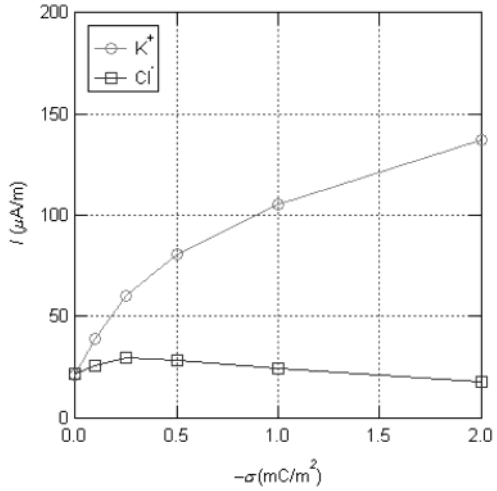

Figure 4. Effect of surface charge density on ionic current. The bulk concentration of KCl aqueous solution is 10^{-4} M and the potential bias is 5 V.

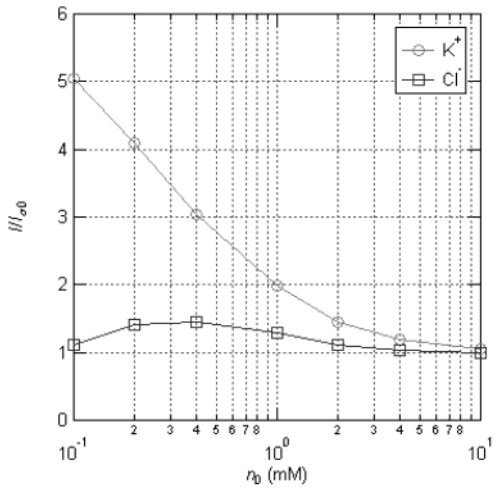

Figure 5. Effect of the bulk concentration of KCl aqueous solution on ionic current. The ionic current of the charged channel, I, is normalized by $I_{\sigma 0}$, which is the current when the surface charge density, $\sigma = 0$. The potential bias is 5 V, and the surface charge densities are -10^{-3} C/m^2.

(b) Effect of Surface Charge Density. To study the effect of surface charge density ionic current, the bulk concentration of KCl aqueous solution is assumed to be 10^{-4} M and the applied potential bias is fixed at 5 V. Figure 4 shows the ionic currents for surface charge densities varying between 0 and -2×10^{-3} C/m^2. As the magnitude of negative surface charge density increases, the ionic current of K^+ increases monotonically, whereas that of Cl^- remains largely unchanged. The main reason for the increase of K^+ current is due to the increase of K^+ concentration inside the channel. But when K^+ ions are accumulated inside the channel, an opposing diffusion current is produced due to a higher concentration gradient. Therefore, the ionic current does not increase proportionally with the ionic density, such that $|\{dI\}/\{d\sigma\}|$decreases with increasing $|\sigma|$.

(c) Effect of Bulk Ion Concentration. Figure 5 shows the ionic current of K^+ and Cl^- as a function of bulk concentration of the KCl aqueous solution under a potential bias of 5 V and surface charge densities of -10^{-3} C/m^2. The ionic current of the charged channel, I, is normalized by that of an uncharged channel, $I_{\sigma 0}$. As the bulk ion concentration increases, the vertical axis, $I/I_{\sigma 0}$, approaches unity, i.e., suggesting that the walls are effectively neutralized by the ions within a length scale much shorter than the channel height, such that the channel behaves like an uncharged one.

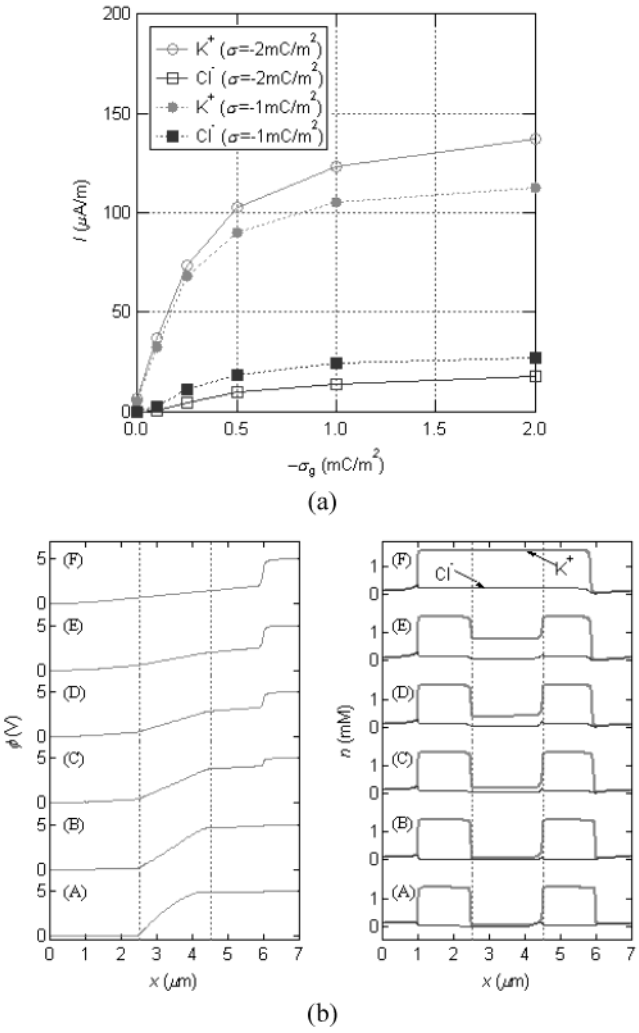

Figure 6. Effect of surface charge density at the gate, σ_g, on ionic current: (a) $I - \sigma_g$ characteristics; (b) electric potential profiles at the center of the channel (left) and ionic density profiles (right) in the channel direction for six different surface charge densities (C/m^2) at the gate, (A) 0, (B) -10^{-4}, (C) -2.5×10^{-4}, (D) -5×10^{-4}, (E) -10^{-3} and (F) -2×10^{-3}. The charge densities on the channel surface except for the gate region are -2×10^{-3} and -10^{-3} C/m^2 (dashed lines in $I-\sigma_g$ characteristics). The bulk concentration of KCl aqueous solution is 10^{-4} M and the potential bias is 5 V.

Gate Effect. To study the effect of a voltage bias on the gate electrode, ion transport was studied under bulk KCl concentration of 10^{-4} M and the potentials at left and right reservoirs are 0 and 5 V, respectively. The surface charge at the gate, σ_g, varied from 0 to -2×10^{-3} C/m^2 and, except for the gate region, the surface charge densities, $\sigma = -10^{-3}$ and -2×10^{-3} C/m^2 were assumed. Figure 6a shows the ionic currents of K^+ and Cl^- as a function of σ_g. The curves are substantially similar to those in Figure 4. For both cases $\sigma = -10^{-3}$ and -2×10^{-3} C/m^2, as $\sigma_g \rightarrow 0$, the ionic current

is blocked almost completely. However, when $\sigma_g \sim \sigma$, the magnitude of the ionic current approaches the value at σ more rapidly in comparison with those in Figure 4, suggesting that the effect of σ_g on the ionic current is nonlinear. The ionic current of Cl^- decreases monotonically with decreasing the surface charge density at the gate, and the value is smaller than that in Figure 4. As σ on the remaining surface increases from -10^{-3} to -2×10^{-3} C/m^2, the unipolar nature of charge transport appears more clearly. To understand the $I-\sigma_g$ behavior, one needs to carefully study the potential and ion concentration distribution, which are shown in Figure 6b along the channel direction. Since the ionic density Cl^- is much smaller than that of K^+ inside the channel, the channel can be considered a unipolar solution. Hence, what is important for ionic current is the distribution of K^+. When σ_g increases from -2×10^{-3} C/m^2 to 0, the K^+ ions are depleted from under the gate such that the concentration drops to that of Cl^-. As a result, most of the potential drop occurs at the gate. Since $\boldsymbol{J}_{K^+}$ is constant along the channel, its value anywhere along the channel is determined by the depleted concentration under the gate. Due to the unipolar nature of charge transport and the effect of gate bias on the charge depletion, and consequently decrease of charge transport, it is fair to compare such as device to that of a metal-oxide-semiconductor field effect transistor (MOSFET).

Conclusions. The Poisson−Nernst−Planck (PNP) equations were used to calculate ionic current along a nanofluidic channel 5 μm long and 30 nm high. The surface charge density ranged from 0 to -2×10^{-3} C/m^2, the bulk concentration of KCl aqueous solution ranged from 10^{-4} to 10^{-2} M, and the potential bias ranged from 0 to 5 V. The following conclusions can be drawn from this study. (1) When the channel size is smaller than the Debye length and the channel surface is charged, the channel becomes a unipolar solution of counterions at a concentration that neutralizes the surface charge. The co-ions are essentially repelled from the channel. (2) Under an applied bias, the ionic current through the nanochannel depends on the surface charge density. (3) As the bulk concentration increases, the ionic current becomes less sensitive to the surface charge density. (4) The current−potential ($I - \phi$) characteristics of the charged channel are nonlinear, which arises from the nonlinear change in the electric field inside the channel with applied electric potential bias. (5) By controlling the surface charge density in a region along the length of the channel, the ion current can be modulated, similar to modulation of charge transport in a field effect transistor due to a gate bias.

Acknowledgment. A.M. thanks the Miller Institute of UC Berkeley for support through a Miller Professorship.

Appendix. The velocity profile due to electroosmotic flow was shown earlier by Burgreen and Nakache.[20] In the case of zero net pressure gradient, the streamwise momentum equation is given by

$$\mu \frac{\partial^2 u}{\partial y^2} = -\rho_e E_x \tag{9}$$

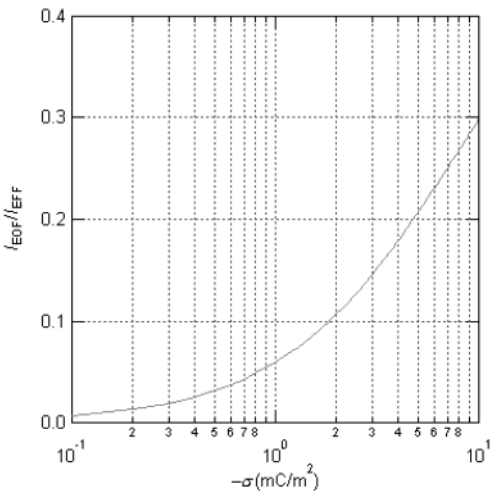

Figure 7. Ratio of the currents due to electroosmotic flow and electrophoretic flow as a function of the surface charge density in the *unipolar* channel of K^+.

where u is the streamwise velocity, μ is the viscosity, ρ_e is the net electric charge density, and $E_x = -\mathrm{d}\phi/\mathrm{d}x$. Using the Poisson equation for ρ_e, we obtain

$$\mu \frac{\partial^2 u}{\partial y^2} = \epsilon_0 \epsilon \frac{\partial^2 \phi}{\partial y^2} E_x \tag{10}$$

The velocity profile is obtained by the integration of eq 10:

$$u(y) = \frac{\epsilon_0 \epsilon E_x}{\mu} \{\phi(y) - \zeta\} \tag{11}$$

where ζ is the zeta potential, the potential at the shear plane at which velocity is zero. If the channel is *unipolar* of K^+, the current due to electroosmotic flow is given by

$$\begin{aligned} I_{EOF} &= \int e n_{K^+}(y) u(y)\, \mathrm{d}y \\ &= \frac{\epsilon_0 \epsilon e E_x}{\mu} \int n_{K^+}(y) \{\phi(y) - \zeta\}\, \mathrm{d}y \end{aligned} \tag{12}$$

From the requirement of electroneutrality, the total charge of ions is equal to the surface charge on the both side walls:

$$-2\sigma = \int e n_{K^+}(y)\, \mathrm{d}y \tag{13}$$

On the other hand, the current due to electrophoretic flow is given by

$$\begin{aligned} I_{EFF} &= \int e n_{K^+}(y) u_{EFF}\, \mathrm{d}y \\ &= -2\sigma \frac{D_K e E_x}{kT} \end{aligned} \tag{14}$$

Figure 7 shows the ratio of the currents due to electroosmotic flow and electrophoretic flow as a function of the surface

charge density in the unipolar channel of K^+. The height of the channel is 30 nm and the viscosity is 10^{-3} Ns/m^2. As the surface charge density increases, the ratio I_{EOF}/I_{EFF} increases. Now the zeta potential of the glass microchannel filled with 10^{-4} M aqueous solution is assumed to be -50 mV.[21] The surface charge density calculated with the Graham equation (eq 6) is -1.34×10^{-3} C/m^2. Note that this surface charge density is the surface charge density of wall plus that of ions within the Stern layer. As the height of the channel decreases less than the Debye length, the density of counterion inside the channel increases, and that inside the Stern layer also increases. Therefore, the surface charge density $|\sigma|$ is estimated to be less than 1.34×10^{-3} C/m^2. In Figure 7, the I_{EOF}/I_{EFF} at $-\sigma = 1.34 \times 10^{-3}$ C/m^2 is 0.07. When the surface charge density $|\sigma|$ is smaller than 2×10^{-3} C/m^2, the I_{EOF}/I_{EFF} is less than about 10 percent.

References

(1) Kasianowicz, J. J.; Brandin, E.; Branton, D.; Deamer, D. W. *PNAS* **1996**, *93*, 13770−13773.
(2) Meller, A.; Nivon, L.; Brandin, E.; Golovchenko, J.; Branton, D. *PNAS* **2001**, *97*, 1079−1084.
(3) Howorka, S.; Cheley, S.; Bayley, H. *Nature Biotechnol.* **2001**, *19*, 636−639.
(4) Li, J.; Stein, D.; McMullan, C.; Branton, D.; Aziz, M. J.; Golovchenko, J. *Nature* **2001**, *412*, 166−169.
(5) Fan, R.; Li, D.; Majumdar, A.; Yang, P. *J. Am. Chem. Soc.* **2003**, *125*, 5254−5255.
(6) Harrison, D. J.; Fluri, K.; Seiler, K.; Fan, Z. H.; Effenhauser, C. S.; Manz, A. *Science* **1993**, *261*, 895−897.
(7) Jacobson, S. C.; Hergenroder, R.; Koutny, L. B.; Ramsey, J. M. *Anal. Chem.* **1994**, *66*, 1114−1118.
(8) Schasfoort, R. B. M.; Schlautmann, S.; Hendrikse, J.; van den Berg, A. *Science* **1999**, *286*, 942−945.
(9) Israelachvili, J. *Intermolecular and Surface Force*, 2nd ed.; Academic Press: London, 1992.
(10) Brett, C. M. A.; Brett, A. M. O. *Electrochemistry, principles, methods, and applications*; Oxford University Press: Oxford, 1993.
(11) Lyklema, J.; Rovillard, S.; Coninck, J. D. *J. Surf. Colloids* **1994**, *14*, 5659−5663.
(12) Qiao, R.; Aluru, N. R. *Nano Lett.* **2003**, *3*, 1013−1017.
(13) Newman, J. S. *Electrochemical Systems*; Prentice-Hall Inc.: Englewood Cliffs, NJ, 1991.
(14) Eisenberg, R. S. *J. Membr. Biol.* **1996**, *150*, 1−25.
(15) Eisenberg, R. S. *J. Membr. Biol.* **1999**, *171*, 1−24.
(16) Klapper, I.; Hagstrom, R.; Fine, R.; Sharp, K.; Honig, B. *Protein: Struct., Funct., Genet.* **1986**, *1*, 47−59.
(17) Kumikova, M. G.; Coalson, R. D.; Graf, P.; Nitzan, A. *Biophys. J.* **1999**, *76*, 642−656.
(18) Hille, B. *Ion channels of excitable membranes*, 3rd ed.; Sinauer Associates Inc.: Sunderland, MA, 2001.
(19) Grahame, D. C. *J. Chem. Phys.* **1953**, *21*, 1054−1060.
(20) Burgreen, D.; Whitehead, R. J. *J. Phys. Chem.* **1964**, *68*, 1084−1091.
(21) Dutta, P.; Beskok, A. *Anal. Chem.* **2001**, *73*, 1979−1986.

NL0348185